ENDOR Determined Molecular Geometries of Spin-Labeled Fluoroanilides in Frozen Solution[1a]

Gregg B. Wells[1b] and Marvin W. Makinen*

Contribution from the Department of Biochemistry and Molecular Biology, The University of Chicago, Cummings Life Science Center, 920 East 58th Street, Chicago, Illinois 60637.
Received November 9, 1987

Abstract: With use of fluorine and proton electron nuclear double resonance (ENDOR) spectroscopy, we have determined the molecular geometries of randomly oriented 2-fluoro-, 3-fluoro-, and 4-fluoroanilide derivatives of the spin-label 2,2,5,5-tetramethylpyrroline-1-oxyl-3-carboxylic acid in frozen perdeuterated methanol. Under conditions of very low modulation depth (3–5 kHz) of the radiofrequency field to ensure that ENDOR line widths were not distorted, ENDOR resonance absorptions were observed specific for the protons and fluorine substituents of the anilide ring. The ENDOR shifts of each fluorine and proton substituent were shown to correspond to principal hyperfine coupling (hfc) components and to exhibit axial symmetry. The ENDOR results also demonstrated that for each fluoroanilide isomer there are two conformers of the anilide ring constrained by the nonbonded 1,6-syn periplanar interactions of an ortho proton or fluorine substituent with the carbonyl oxygen. The electron–nucleus separations were calculated from the dipolar hfc contributions according to the point–dipole, strong-field approximation. Assignments of the resonance frequencies of ENDOR features were confirmed on the basis of spectral simulations. To assess the accuracy of this method of deriving structural details from ENDOR spectra of molecules in frozen solutions, we have compared the ENDOR-determined electron–nucleus separations with those predicted through computer-based molecular graphics modeling of X-ray-derived atomic coordinates of the spin-label and fluoroanilide moieties covalently bonded through a planar amide group. With assignment of the effective dipole of the nitroxyl group to the midpoint of the N–O bond, there was less than a 5% discrepancy between the ENDOR-determined and molecular model results for electron–nucleus distances over a 5–11-Å range. The ENDOR and molecular modeling results demonstrated that the fluorines and protons of the anilide group are essentially coplanar with the pyrrolinyl ring, the maximum deviation of the electron–nucleus vector from the molecular plane of the spin-label being less than 21°. This application of ENDOR spectroscopy to nitroxide spin-labels provides a basis for a general method to determine detailed molecular geometries of spin-labeled molecules in frozen solution.

Since the first demonstration of electron nuclear double resonance,[2] this spectroscopic technique has been widely applied to characterize paramagnetic sites in solids and liquids. The electron spin interacts with magnetic nuclei in its nearby environment through dipolar and contact interactions, producing shifts in their resonance frequencies. ENDOR[3] spectra of solid samples, obtained by partially saturating an EPR transition and sweeping a radiofrequency field through nuclear resonance transitions, can be analyzed to yield the dipolar contributions and to determine nuclear coordinates. While these objectives are readily achieved in single-crystal studies,[4,5] the application of ENDOR to amorphous or polycrystalline systems has generally relied on systems with anisotropic g values to take advantage of the angular selection of molecular orientations with respect to the static laboratory magnetic field.[6-8] Under such conditions, the larger the anisotropy, the better resolved is the selection of a given orientation of the paramagnetic species.

The nitroxyl free-radical species known as spin-labels are chemically stable, magnetically well-behaved, and widely employed in biophysical studies as spectroscopic probes of macromolecular structure.[9-12] The use of these free-radical probes has been directed largely toward only a qualitative evaluation of equilibrium binding effects and changes in conformational flexibility. Direct structural information in terms of stereochemical and steric interactions has generally not been achieved except for a relatively small number of single-crystal EPR studies to determine spin-label orientation and conformation[13-15] or except for studies to estimate the radial separation between the nitroxyl group and immobilized paramagnetic cations.[16,17] The magnetic interactions in the nitroxyl group are characterized in general by nearly isotropic g values and anisotropic hyperfine coupling with the nitrogen nucleus.[18-21] Consequently, it would appear that nitroxyl spin-

(1) (a) This work was supported by grants of the National Institutes of Health (GM 21900 and AA 06374). (b) Supported in part by an MSTP Training Grant of the National Institutes of Health (GM 07281).
(2) (a) Feher, G. *Phys. Rev.* **1956**, *103*, 834–835. (b) Feher, G. *Ibid.* **1959**, *114*, 1219–1244.
(3) The following abbreviations are used: CDI, 1,1'-carbonyldiimidazole; ENDOR, electron nuclear double resonance; EPR, electron paramagnetic resonance; hf, hyperfine; hfc, hyperfine coupling; rf, radiofrequency.
(4) (a) Hutchison, C. A., Jr.; McKay, D. B. *J. Chem. Phys.* **1977**, *66*, 3311–3330. (b) Hutchison, C. A., Jr.; Orlowski, T. E. *Ibid.* **1980**, *73*, 1–14. (c) Fields, R. A.; Hutchison, C. A., Jr. *Ibid.* **1985**, *82*, 1712–1722.
(5) (a) de Beer, R.; de Boer, W.; van't Hof, C. A.; van Ormondt, D. *Acta Crystallogr. Sect. B* **1973**, *29*, 1473–1480. (b) Atherton, N. M.; Horsewill, A. J. *J. Chem. Soc., Faraday Trans. 2* **1980**, *76*, 660–666.
(6) (a) Rist, G. H.; Hyde, J. S. *J. Chem. Phys.* **1970**, *52*, 4633–4643. (b) Schweiger, A. *Struct. Bonding (Berlin)* **1982**, *51*, 1–28.
(7) (a) Hurst, G. C.; Henderson, T. A.; Kreilick, R. W. *J. Am. Chem. Soc.* **1985**, *107*, 7294–7299. (b) Henderson, T. A.; Hurst, G. C.; Kreilick, R. W. *Ibid.* **1985**, *107*, 7299–7303.
(8) (a) Hoffman, B. M.; Martinsen, J.; Venters, R. A. *J. Magn. Reson.* **1984**, *59*, 110–123. (b) Hoffman, B. M.; Venters, R. A.; Martinsen, J. *Ibid.* **1985**, *62*, 537–542.
(9) Hamilton, C. L.; McConnell, H. M. In *Structural Chemistry and Molecular Biology*; Rich, A., Davidson, N., Eds.; W. H. Freeman: San Francisco, 1968; pp 115–149.
(10) McConnell, H. M.; Gaffney-McFarland, B. *Q. Rev. Biophys.* **1970**, *3*, 91–136.
(11) Berliner, L. J., Ed.; *Spin Labeling: Theory and Application*; Academic Press: New York, 1976; pp 592.
(12) Jost, P. C.; Griffith, O. H. *Methods Enzymol.* **1978**, *49*, 369–418.
(13) (a) McConnell, H. M.; Hamilton, C. L. *Proc. Natl. Acad. Sci. U.S.A.* **1968**, *6*, 776–781. (b) Chien, J. C. W. *J. Mol. Biol.* **1979**, *133*, 385–398.
(14) (a) Berliner, L. J.; McConnell, H. M. *Biochem. Biophys. Res. Commun.* **1971**, *43*, 651–657. (b) Bauer, R. S.; Berliner, L. J. *J. Mol. Biol.* **1979**, *128*, 1–19.
(15) (a) Chien, J. C. W.; Dickinson, L. C. In *Biological Magnetic Resonance*; Berliner, L. J., Reuben, J., Eds., Plenum Press: New York, 1981; Vol. 3, pp 55–212. (b) Makinen, M. W.; Kuo, L. C. In *Magnetic Resonance in Biology*; Cohen, J. S., Ed. Wiley: New York, 1983; Vol. 2, pp 53–94.
(16) Leigh, J. S. *J. Chem. Phys.* **1970**, *52*, 2608–2612.
(17) (a) Morrisett, J. D. In *Spin Labeling: Theory and Applications*; Berliner, L. J., Ed.; Academic Press: New York, 1976; pp 273–338. (b) Berliner, L. J. *Methods Enzymol.* **1978**, *49*, 418–480.
(18) Griffith, O. H.; Cornell, D. W.; McConnell, H. M. *J. Chem. Phys.* **1965**, *43*, 2909–2910.
(19) Capiomont, A.; Chion, B.; Lajzerowicz-Bonneteau, J.; Lemaire, H. *J. Chem. Phys.* **1974**, *60*, 2530–2535.
(20) (a) Brustolon, M.; Maniero, A. L.; Segre, U. *Mol. Phys.* **1985**, *55*, 713–321. (b) Brustolon, M.; Maniero, A. L.; Segre, U.; Greci, L. *J. Chem. Soc., Faraday Trans.* **1987**, *83*, 69–75.
(21) Brustolon, M.; Maniero, A. L.; Corvaja, C. *Mol. Phys.* **1984**, *51*, 1269–1281.

0002-7863/88/1510-6343$01.50/0

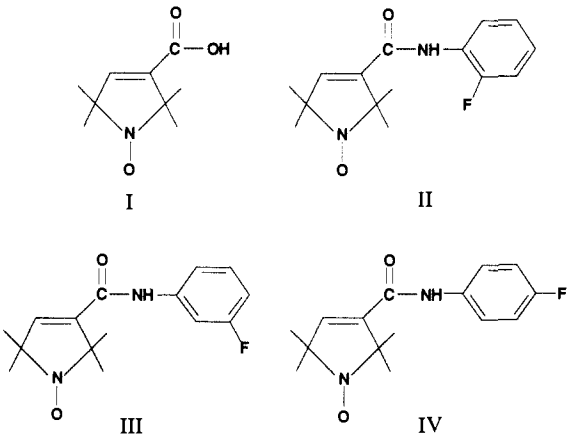

Figure 1. Illustration of the chemical bonding structure of 2,2,5,5-tetramethylpyrroline-1-oxyl-3-carboxylic acid (I) and of its ortho-, meta-, and para-substituted fluoroanilide derivatives II–IV.

labels are unsuitable as probes of molecular structure for ENDOR studies. Furthermore, because of the chemical bonding structure with four nearby methyl groups that underlie the chemical stability of the nitroxyl group in solution, there is a high density of protons in the immediate environment of the free radical.

We report the results of a detailed ENDOR study of spin-labeled fluoroanilides in frozen solution, demonstrating that ENDOR resonances specific for ^{19}F and ^{1}H nuclei on the anilide ring can be detected and that estimates of electron–nucleus separations from the nitroxyl group to substituents not directly bonded to the spin-label moiety can be made with high accuracy. The series of isomeric spin-labeled fluoroanilides chosen for this investigation is illustrated in Figure 1. This series was employed under the expectation that the conformation of the anilide ring is geometrically constrained through conjugation of the aromatic group with the amide bond and the olefinic bond of the pyrrolinyl ring. The ENDOR spectra show that resonances for the anilide substituents are attributable to two different conformations of the aromatic ring derived by rotation about the anilide C–N bond and constrained by the steric interactions of the carbonyl oxygen with the substituents at the ortho positions of the anilide ring. The spectroscopically determined distances agree to within ±5% with results obtained by computer-based molecular modeling. On this basis, we demonstrate that ENDOR spectroscopy of nitroxyl spin-labels provides a general method of structure determination of molecules in frozen solutions through measurement of electron–nucleus distances in the 5- to 11-Å range and with an accuracy that is exceeded probably only by that associated with single-crystal diffraction methods.

Experimental Procedures

Materials. The spin-label 2,2,5,5-tetramethylpyrroline-1-oxyl-3-carboxylic acid (I) was obtained from Molecular Probes, Inc. (Eugene, OR 97402), or was synthesized according to the method of Rozantsev.[22] Ortho-, meta-, and para-substituted fluoroanilines and 1,1-carbonyldiimidazole (CDI) were obtained from Aldrich Chemical Co. (Milwaukee, WI 53233) and were used without further purification. Methanol-d_4 was obtained from Cambridge Isotope Laboratories (Woburn, MA 01801). All other chemicals were of analytical reagent grade. Deionized, distilled water was used throughout. Organic solvents were dried over molecular sieves.

Compounds II–IV were synthesized with CDI as the coupling reagent. As a typical procedure 0.25 g (0.00136 mol) of I and 0.23 g (0.00143 mol) of CDI were dissolved in 15 mL of dry CH_2Cl_2. After approximately 15 min, 0.152 g (0.00137 mol) of *o*-, *m*-, or *p*-fluoroaniline was added. The reaction mixture was stirred for 48 h at room temperature and was extracted four times with 100 mL of 0.1 N HCl and two times with 100 mL of 5% (w/v) $NaHCO_3$, followed by washing to neutrality with distilled water and drying over $MgSO_4$. Removal of the CH_2Cl_2 in vacuo left a yellow solid which was recrystallized from a mixture of acetone and petroleum ether. Yields were 26, 40, and 53% of theoretical for II, III, and IV, respectively. For $C_{15}H_{18}N_2O_2F$ with a theoretical percentage elemental composition of C (64.97), H (6.54), N (10.10), and F (6.85), the following analyses were obtained for each isomeric fluoroanilide. II: mp 106–107 °C; C (64.41), H (6.18), N (10.17), F (7.37). III: mp 203–205 °C; C (64.81), H (6.61), N (10.08), F (6.61). IV: mp 187–189 °C; C (64.67), H (6.54), N (10.13), F (6.90).

EPR and ENDOR. Spectra were recorded at 40 K with an X-band Bruker ER200D spectrometer equipped with an Oxford Instruments ESR10 liquid helium cryostat and a Bruker digital ENDOR accessory, as previously described.[23,24] The microwave frequency was determined with a Hewlett-Packard 5350A frequency counter. ENDOR spectra were recorded in the first-derivative absorption mode with 1.28 mW incident microwave power, 12.5 kHz modulation of the rf field, and 50 W rf power with less than 10 kHz modulation depth of the rf field. The latter is a particularly important condition to eliminate the matrix ENDOR signal and to achieve the spectral resolution described in this investigation for resonances within 0.5 MHz of their respective free nuclear frequencies. The static laboratory magnetic field was not modulated for ENDOR. Each spin-labeled fluoroanilide was dissolved to a concentration of 5 mM in CD_3OD for spectroscopic studies and frozen at the temperature of liquid nitrogen, producing a glass-like sample. All ENDOR spectra are presented as single scan recordings with use of the longest sweep time possible because of our lack of signal averaging facilities.

Molecular Modeling. The structures of spin-labeled fluoroanilides were constructed on the basis of molecular fragments. The atomic coordinates of the nonhydrogen atoms of the spin-label moiety, including the carbon, oxygen, and nitrogen of the amide bond, were taken from the X-ray study of 2,2,5,5-tetramethylpyrroline-1-oxyl-3-carboxamide,[25] and the positions of the nonhydrogen atoms of the fluoroaniline moiety were based on the X-ray defined structures of *p*-chloroaniline,[26] *trans*-dichloro-bis(*p*-fluoroaniline)palladium(II),[27] and acetanilide.[28] Positions of fluorine and hydrogen atoms on the aromatic rings of II–IV were calculated for idealized geometries using F–C–C and H–C–C bond angles of 120°, a C–F bond length of 1.30 Å, and a C–H bond length of 1.08 Å.[29] Because of the partial double bond character of the C–N bond of the amide group, we imposed a planar geometry around the amide nitrogen, with a C–N–C angle of 120°. This structural constraint leaves only one intramolecular degree of freedom in the anilide, i.e., rotation about the N–C bond of the fluoroaniline moiety. The extent of rotation is measured by the dihedral angle χ between the plane formed by the carbon, oxygen, and nitrogen, and hydrogen of the amide group and the plane of the aromatic ring. The models were analyzed with the programs FRODO[30] and SYBYL,[31] running on an Evans and Sutherland PS330 molecular graphics system with a host Digital Electronics Corp. VAX 11/750 computer.

Theory

EPR of Nitroxyl Spin-Labels. We restrict the discussion of the EPR of nitroxyl spin-labels to those aspects that are important for understanding the ENDOR results. The Hamiltonian in eq 1 describes the EPR spectrum of spin-labels including hf inter-

$$\mathcal{H} = |\beta_e|\mathbf{H}_0\cdot\mathbf{g}_e\cdot\mathbf{S} - |\beta_n|g_n\mathbf{H}_0\cdot\mathbf{I} + \mathbf{S}\cdot\mathbf{A}\cdot\mathbf{I} \qquad S = \tfrac{1}{2},\ I = 1 \qquad (1)$$

action of the unpaired electron with the nitrogen nucleus of the nitroxyl group.[9,18] In eq 1, S is the electron spin operator, **I** is the nitrogen nuclear spin operator, $\mathbf{g}_e$ is the electronic Zeeman interaction matrix, g_n and β_n are the nuclear g value and magneton,

(22) Rozantsev, E. G. *Free Nitroxyl Radicals*; Plenum Press: New York, 1970; Chapter 9, pp 203–246.

(23) (a) Yim, M. B., Kuo, L. C.; Makinen, M. W. *J. Magn. Reson.* **1982**, *46*, 247–256. (b) Makinen, M. W.; Kuo, L. C.; Yim, M. B.; Wells, G. B.; Fukuyama, J. M.; Kim, J. E. *J. Am. Chem. Soc.* **1985**, *107*, 5245–5255.

(24) Yim, M. B.; Makinen, M. W. *J. Magn. Reson.* **1986**, *70*, 89–105.

(25) Turley, J. W.; Boer, F. P. *Acta Crystallogr., Sect. B* **1972**, *28*, 1641–1644.

(26) Ploug-Sørensen, G.; Andersen, E. K. *Acta Crystallogr., Sect. C* **1985**, *41*, 613–615.

(27) Padmanabhan, V. M.; Patel, R. P.; Ranganathan, T. N. *Acta Crystallogr., Sect. C* **1985**, *41*, 1305–1307.

(28) (a) Brown, C. K.; Corbridge, D. E. *Acta Crystallogr.* **1954**, *7*, 711–715. (b) Brown, C. J. *Ibid.* **1966**, *21*, 442–445.

(29) Kennard, O. In *International Tables for X-ray Crystallography*; MacGillavry, C. H., Rieck, G. D., Eds.; Kynoch Press, Birmingham, U.K., 1968; Vol. 3, Section 4.2, pp 275–276.

(30) (a) Jones, T. A. In *Computational Crystallography*; Sayre, D., Ed.; Clarendon Press: Oxford, 1982; pp 303–317. (b) Jones, T. A. *Methods Enzymol.* **1985**, *115*, 157–171.

(31) Marshall, G. R., personal communication. Detailed information on the use of this program package can be obtained from Tripos Associates, Inc. 6548 Clayton Rd., St. Louis, MO 63117.

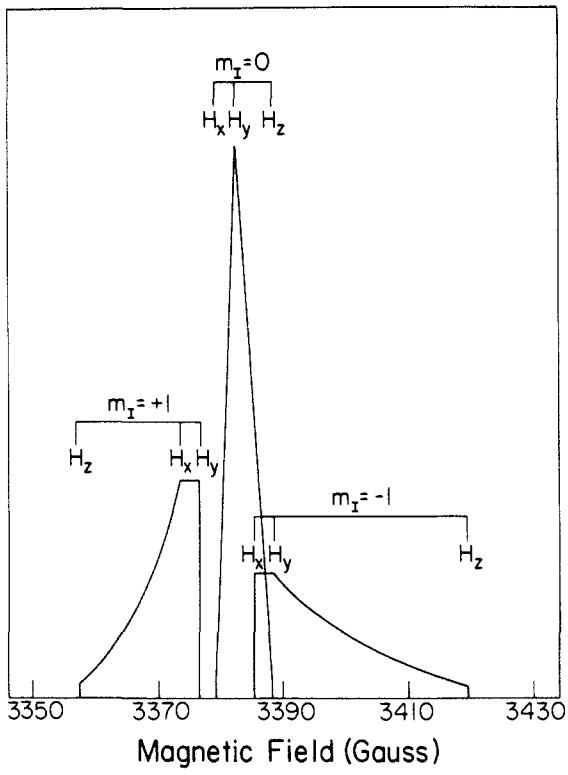

Figure 2. Schematic diagram of the EPR absorption spectrum of a collection of randomly oriented nitroxyl spin-label molecules with ^{14}N hf coupling. The spectrum is composed of contributions from three species which are distinguished by the value of m_I. Molecules with $m_I = 0$ show the narrowest range of magnetic field as a function of orientation for resonance. This circumstance indicates that there is little orientational selectivity of molecules as a function of $\mathbf{H}_0$ applied to this resonance absorption region. This region, thus, provides the closest approximation to an isotropic EPR spectrum. The diagram is patterned according to Lee et al.[33] The parameters used for this diagram are the following: microwave frequency, 9.5 GHz; $g_{xx} = 2.0086$, $g_{yy} = 2.0066$, $g_{zz} = 2.0032$; $A_{xx} = A_{yy} = 6$ G; $A_{zz} = 31$ G with coincident principal magnetic axes of the g-value and hf interaction matrices, as determined for 2,2,5,5-tetramethylpyrroline-1-oxyl-3-carboxamide,[19] which we have used as a model for these spectroscopic studies. We designate for ENDOR experiments the condition of microwave saturation at H_z of the $m_I = +1$ region as setting A while microwave saturation of the $m_I = 0$ region is designated as setting B.

respectively, β_e is the Bohr magneton, and $\mathbf{A}$ is the electron–nuclear hf interaction matrix. The nitroxyl group and the four carbon atoms of the pyrrolinyl ring are coplanar according to X-ray studies.[25,32] We assume also for compounds II–IV that all atoms of the five-membered ring are similarly coplanar with the nitroxyl oxygen because of the olefinic bond.

The EPR spectrum of nitroxyl spin-labels can be considered as a composite of spectra from three different sets of molecules, differing by their projection of the ^{14}N nuclear moment onto the laboratory magnetic field $\mathbf{H}_0$ and designated by the values of m_I, as illustrated systematically in Figure 2. The features at the low-field and high-field regions of the spectrum arise from molecules with $m_I = +1$ and $m_I = -1$, respectively, while the intense, central features arises predominantly from molecules with $m_I = 0$. The EPR spectrum from this set of molecules shows less anisotropy than do molecules with $m_I = \pm 1$. Consequently, the values of $\mathbf{H}_0$ corresponding to alignment along g_{xx} and g_{zz} that define the low-field and high-field limits of the central absorption feature differ by only 9.1 G at the microwave frequency of 9.48 GHz employed in our experiments. For this reason microwave power saturation at the central region of the EPR absorption spectrum selects a collection of essentially randomly oriented molecules with $m_I = 0$. On the other hand, microwave power saturation at the low-field or high-field limits with $m_I = \pm 1$ selects molecules for ENDOR with the plane of the pyrrolinyl ring oriented perpendicular to $\mathbf{H}_0$. The strategy for obtaining electron–nuclear distances by ENDOR spectroscopy of nitroxyl spin-labels in this investigation relies on this region with unresolved, overlapping absorption due to low g anisotropy. We designate this approach as the isotropic approximation.

ENDOR of Nitroxyl Spin-Labels. In the special case of a system of low g anisotropy within the strong-field approximation, as obtains for nitroxyl spin-labels, the ENDOR transitions of frequency $\nu_\pm$ of a nucleus are symmetric to first order about the free nuclear frequency ν_n according to the eq:

$$\nu_\pm = \nu_n \pm |A|/2 \tag{2}$$

where A represents an orientation dependent value of the hf coupling. Under the condition that $\mathbf{H}_0$ is applied parallel to the principal axis i of the hf interaction matrix, this becomes identical with the corresponding principal hfc component A_{ii}. The separation of $\nu_\pm$ about ν_n is called the ENDOR shift; for symmetric separations the hf coupling is, thus, twice the value of this frequency spacing.

Within the point–dipole approximation, the value of the observed hf coupling A is given by eq 3 as a function of r and α,

$$A = \frac{g_n|\beta_n|g_e|\beta_e|\ (3\cos^2\alpha - 1)}{hr^3} + A_{iso} \tag{3}$$

where r is the modulus of the position vector r beteen the electron and the nucleus, α is the angle between $\mathbf{H}_0$ and r, g_e is the effective electronic g value (defined below), and A_{iso} is the isotropic hfc constant. The principal hfc components due to dipole–dipole interaction $A_\parallel^D$ and $A_\perp^D$ correspond to the first term on the right-hand side of eq 3 for values of $\alpha = 0$ and 90°, respectively. Under the condition that $A_{iso} \ll A_\parallel$ and $A_\perp$, then $A_\parallel^D > 0 > A_\perp^D$, and the hfc constants $A_\parallel^D$, $A_\perp^D$ and A_{iso} are calculated under the constraint $(A_\parallel + 2A_\perp)/3 = A_{iso}$. We shall show that the observed ENDOR shifts of the spin-labeled fluoroanilides employed in this study are almost entirely accounted for by dipolar interactions and that the isotropic contribution is very small. Since the pseudo-contact contribution[34] to the isotropic hfc is negligible in view of the very low g anisotropy of nitroxyl spin-labels,[2,18,19] we do not distinguish further between this component and the Fermi contact term that comprise A_{iso}.

We evaluate the quantitative limits of application of eq 3 to nitroxyl spin-labels. Firstly, the accuracy of the strong-field approximation improves as the g factor anisotropy decreases. Following Hutchison and McKay,[4a] we evaluate the expectation value of the electronic magnetic moment associated with the unpaired electron of the nitroxyl group by eq 4 in which $\mathbf{g}_e$ is

$$\langle\mu_e\rangle_\pm = -|\beta_e|\ \mathbf{g}_e \cdot \langle S\rangle_\pm = -\frac{|\beta_e|}{2g_e}\begin{bmatrix} g_{xx}^2 & l_1 \\ g_{yy}^2 & l_2 \\ g_{zz}^2 & l_3 \end{bmatrix} \tag{4}$$

considered as a diagonalized matrix, the quantity $\langle S\rangle_\pm$ is the expectation value of $\mathbf{S}$, the l_i are the direction cosines of $\mathbf{H}_0$ in the molecular axis system, and g_e is the effective value of $\mathbf{g}_e$ defined by the relation $g_e = [l_1^2 g_{xx}^2 + l_2^2 g_{yy}^2 + l_3^2 g_{zz}^2]^{1/2}$. The extreme principal values g_{xx} and g_{zz} of the model spin-label system differ by only 0.28%.[18,19] On this basis, if we apply g as the average value of g_{xx}, g_{yy}, and g_{zz}, then $\langle\mu_e\rangle_\pm \approx -|\beta_e|g/2$. Secondly, the accuracy of the strong-field approximation increases with increasing r. For a spin system with $g = 2.006$ at 3500 G, the maximum magnetic field $\mathbf{h}_e$ generated at an electron–nucleus separation of 5 Å is ~150 G. This value is small compared to that of the applied laboratory magnetic field $\mathbf{H}_0$ and will be less

(32) Boeyens, J. C. A.; Kruger, G. J. *Acta Crystallogr., Sect. B* **1970**, *26*, 668–672.
(33) Lee, S.; Ames, D. P.; Putnam, J. M. *J. Magn. Reson.* **1982**, *49*, 312–321.
(34) (a) McConnell, H. M.; Chestnut, D. B. *J. Chem. Phys.* **1958**, *28*, 107–117. (b) McConnell, H. M.; Robertson, R. E. **1958**, *29*, 1361–1365.

for larger values of r. Correspondingly, the maximum angle between $\mathbf{H}_0$ and the effective field ($\mathbf{H}_0 \pm \mathbf{h}_e$) at the nucleus is 2.0° for $\alpha = 45°$. This angle is 0° for $\alpha = 0$ or 90°, the orientations that give rise to ENDOR features corresponding to $A_\parallel$ and $A_\perp$, respectively. Thirdly, the accuracy of the point-dipole approximation improves with increasing values of r. For a nucleus at $r = 5$ Å, we can evaluate the error in applying the point-dipole approximation for a nitroxyl group according to a McConnell-Strathdee calculation.[35] For an effective nuclear charge Z ranging from 3.5 to 4.5 and with all of the spin density localized in a pπ-type orbital of the nitrogen, the deviation of the hfc constants from the values obtained under the point-dipole approximation ranges from 4.9 to 3.0%. This deviation decreases as r increases. Thus, the point-dipole and strong-field approximations contribute less than 5% error to estimates of the principal dipolar hfc components. In view of the $1/r^3$ dependence of the electron-nucleus separation on the hfc, the effect is to contribute less than 3% error to estimates of $r \geq 5$ Å. These errors are smaller than the errors associated with the assignment of the values of the ENDOR shifts of nuclei on the anilide group on the basis of ENDOR spectra, as described in this investigation.

In order to compare ENDOR determined values of r with corresponding distances derived from molecular modeling, it is necessary to assign coordinates for the electronic point-dipole of the nitroxyl group. As a first-order approximation we assign the coordinates r_e of the *effective* electronic point dipole along the N-O bond in vew of the highly localized distribution of the unpaired spin to the nitroxyl group.[9,10,19,36] Since the distribution of spin density is influenced by the polarity of the solvent[12,37] and the error from the assignment of the effective coordinates will depend on the geometrical relationships of the nucleus to the nitroxyl group, we vary r_e between the nitroxyl nitrogen and oxygen according to the equation:

$$r_e = \rho_N r_N + \rho_O r_O \qquad (5)$$

where r_N is the position vector of the nitroxyl nitrogen and r_O is the position vector of the oxygen atom and the ρ's represent the corresponding spin densities. For densities ranging between 0.8 to 0.5 on the nitrogen and between 0.2 to 0.5 on the oxygen,[19,33] a maximum error of 0.38 Å is introduced for a nucleus colinearly positioned with the N-O bond. For all other geometries the error is less, and for a nucleus at a distance of $r \geq 5$ Å the relative error is very small. Furthermore, according to the equation[38] $A_{iso} = \rho_N Q_N + \rho_O Q_O$ and measured values of the nitrogen isotropic hfc in solvents of extreme polarity,[39] we estimate that r_e should shift no more than 0.15 Å along the N-O bond for corresponding changes in solvent environment.

Simulation of ENDOR Spectra. To interpret ENDOR spectra, we have developed a calculation program to simulate ENDOR spectra in disordered rigid media, following the model of Brustolon et al.[20] specific for nitroxyl spin-labels. Simulation of spectra is carried out by summing discrete Lorentzian functions each representing the resonance signals from an individual nuclear spin-packet, for which the maxima occur at the value of the ENDOR shift calculated according to eq 2 and 3 for dipolar interactions only. The origin is placed at the point-dipole of the unpaired electron spin and the x,y plane corresponds to that defined in the nitroxyl spin-label. For a uniform distribution of molecules with all orientations of r over the 4π steradian solid angle of a unit sphere, the contribution of a given orientation of the nitroxyl group to the ENDOR spectrum will be weighted by a function of the magnetic field setting $\mathbf{H}_0$ at which saturating levels of microwave power are applied to the spin system. We anticipate on this basis that the summed contributions will give rise to line shapes differing from those of a single orientation when the weighting function provides poor selectivity for orientations of r. We also assume that the ENDOR signal amplitude is independent of the orientation of r with respect to $\mathbf{H}_0$. Simulated ENDOR spectra were then obtained for model systems with an isotropic or an axially symmetric g matrix according to the equation

$$I(\nu) = \sum_{m_s}\sum_{\phi}\sum_{\theta} w(\theta)\left[\frac{\Gamma^2}{\Gamma^2 + (\nu - \nu_{m_s}(\theta,\phi))^2}\right]\sin\theta \qquad (6)$$

where $I(\nu)$ is the intensity at frequency ν relative to the free nuclear frequency; $w(\theta)$ is a weighting function, unity for simulations of isotropic g systems and Gaussian for simulations of axially symmetric g systems (vide infra); Γ is one-half of the line width at half-maximum height of the Lorentzian function that describes the ENDOR signal for each orientation; and $\nu_{m_s}(\theta,\phi)$ is the ENDOR shift calculated on the basis of eq 2 and 3 where θ and ϕ represent polar and azimuthal angles, respectively. For a set of randomly oriented molecules in a unit sphere, the ENDOR shifts were calculated for all orientations of r at 0.5° intervals in ϕ and at 1.0° intervals in θ. The influence of an axially symmetric g matrix was incorporated into the simulations by weighting the contribution of each orientation by the Gaussian function given in eq 7, where $\bar{\nu}$ is the microwave frequency of the spectrometer

$$w(\theta) = \frac{1}{\sigma(2\pi)^{1/2}}\exp[-(\bar{\nu} - \bar{\nu}(\theta))^2/2\sigma^2] \qquad (7)$$

and $\bar{\nu}(\theta) = |\beta_e|\mathbf{H}_0 g(\theta)/h$ where $g(\theta) = [g_\parallel^2\cos^2\theta + g_\perp^2\sin^2\theta]^{1/2}$, θ being the angle between the direction of $\mathbf{H}_0$ and the symmetry axis of $\mathbf{g}_e$. The parameter σ has a preset value corresponding to the single-crystal EPR line width[20] and represents the standard deviation of the Gaussian weighting function.

Our objective is to relate the shape and frequency of absorption in first-derivative ENDOR spectra to the values of the principal hfc components due to dipolar interactions since the latter can be precisely calculated for a model system according to eq 3. The salient results of these spectral simulations are illustrated in Figure 3 and are obtained with a value for σ of 5 MHz. This value represents a realistic lower limit of the single-crystal EPR line width.[10,20,21] These simulated ENDOR spectra are of a fluorine nucleus interacting with a spin system characterized by an axially symmetric g-value matrix. Comparable results are obtained for a system with an isotropic g.[40] In Figure 3 it is seen that the ENDOR shift corresponding to $-A_\parallel/2$ coincides with the position of the maximum of the outermost ENDOR band in a first-derivative spectrum. On the other hand, the ENDOR shift corresponding to $A_\perp/2$ coincides with a point on the inner portion of the first-derivative trace of the innermost ENDOR resonance feature. It is noteworthy that the value of the ENDOR shift in the latter case coincides neither with an inflection point nor with a point midway between the maximum and minimum of the trace. For simulations with an isotropic g, increasing the parameter Γ representing the line width of the Lorentzian function obscured the features in the spectrum but did not alter their position.[40] Although the relative intensities of the parallel and perpendicular ENDOR features differ for isotropic and anisotropic cases, the ENDOR shifts do not change for values of $\sigma \geq 5$ MHz. We have based our assignments of the values of ENDOR shifts on these general guidelines illustrated in Figure 3.

It is of interest to note that the relationships between the shapes of the ENDOR resonance features and the positions of the ENDOR shifts for parallel and perpendicular absorptions in the first-derivative spectrum are analogous to those between the shape of an axially symmetric first-derivative EPR spectrum and its principal g values.[41-43] For a spin system with axially symmetric

(35) McConnell, H. M.; Strathdee, J. *Mol. Phys.* **1959**, *2*, 129-138.
(36) (a) Davis, T. D.; Christoffersen, R. E.; Maggiora, G. M. *J. Am. Chem. Soc.* **1975**, *97*, 1347-1354. (b) Kikuchi, O. *Bull. Chem. Soc. Jpn.* **1969**, *42*, 47-52. (c) Kikuchi, O. *Ibid.* **1969**, *42*, 1187-1191.
(37) Griffith, O. H.; Dehlinger, P. J.; Van, S. P. *J. Membrane Biol.* **1974**, *15*, 159-192.
(38) Karplus, M.; Fraenkel, G. K. *J. Chem. Phys.* **1961**, *35*, 1312-1323.
(39) Cohen, A. H.; Hoffman, B. M. *J. Am. Chem. Soc.* **1973**, *95*, 2001-2002.
(40) Wells, G. B. Ph.D. Thesis, The University of Chicago, 1987, pp 254.
(41) Kneubühl, F. K. *J. Chem. Phys.* **1960**, *33*, 1074-1078.
(42) Atkins, P. W.; Symons, M. C. R. *The Structure of Inorganic Radicals*; Elsevier: New York, 1967; Appendix 5, pp 268-272.

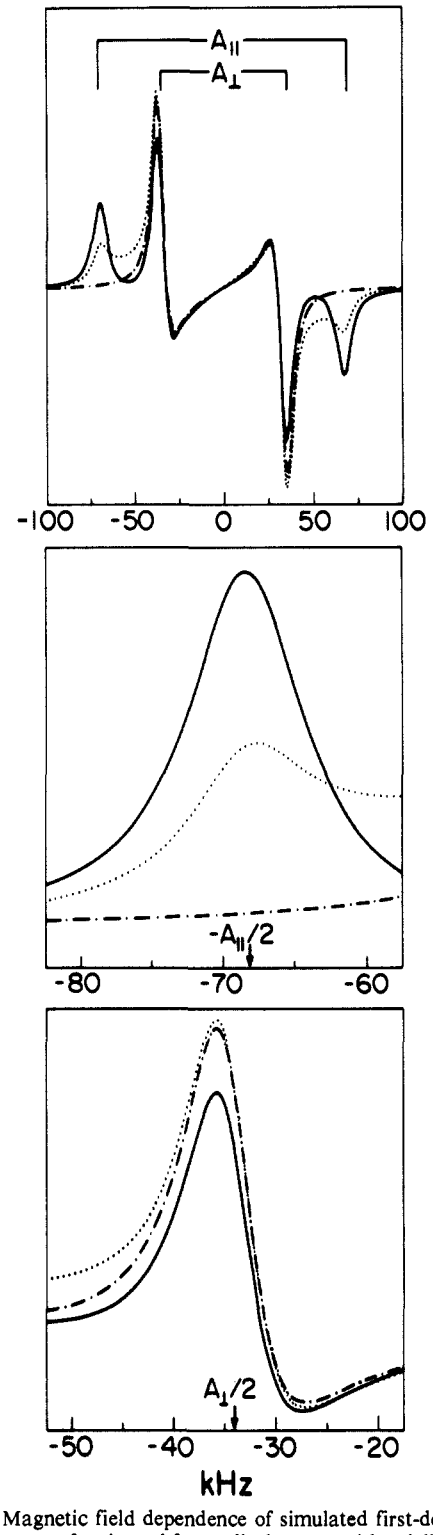

Figure 3. Magnetic field dependence of simulated first-derivative ^{19}F ENDOR spectra of a nitroxyl free radical system with axially symmetric principal g values. Top panel: ENDOR spectra of a fluorine nucleus coincident with the molecule x,y plane. A value for Γ of 5 kHz was used for spectral simulation. The spectra correspond to saturation at g_e values of 2.0090 (90°, —), 2.0075 (60°; ···), and 2.0045 (30°, -·-) where the values of the angles θ are calculated from $g_e^2 = [g_\parallel^2 \cos^2\theta + g_\perp^2 \sin^2\theta]$. The parallel features, prominent for $\theta \approx 90$ and 75°, show reduced intensity at $\theta \approx 60°$ and are barely detectable at $\theta \simeq 45°$. Positioning the fluorine in the x,y plane causes the perpendicular features to be present at all values of θ. Central panel: Comparison of ENDOR absorption features for one of the parallel ($A_\parallel$) hfc components. The maximum in the trace closely corresponds to $-A_\parallel/2$. Bottom panel: Comparison of the spectral feature for one of the perpendicular ($A_\perp$) hfc components. A position on the innermost side of the ENDOR band corresponds to the value of $A_\perp/2$. The parameters used to calculate the spectra are r = 10.3 Å, $g_\parallel$ = 2.009, $g_\perp$ = 2.003, σ = 5.0 MHz, $A_\parallel$ = 136.37 kHz, and $A_\perp$ = 68.18 kHz.

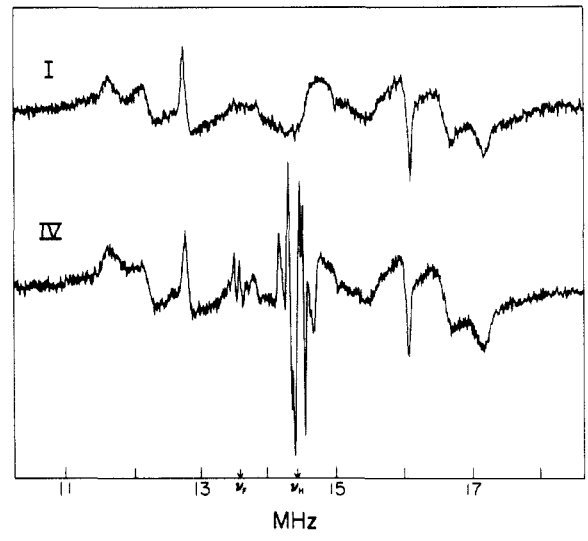

Figure 4. Identification of ENDOR spectral features belonging to the fluorine and protons of the fluoroanilide ring of IV: top, spectrum of I; bottom, spectrum of IV. These spectra were taken with $\mathbf{H}_0$ applied to position B of the EPR spectrum of the nitroxide group (see Figure 2). The free fluorine and free proton Larmor frequencies ν_F and ν_H are indicated by arrows. Features that appear in both spectra arise from the methyl and vinylic protons of the spin-label and exhibit ENDOR shifts greater than 0.5 MHz, leaving the region close to ν_H unobscured. The numerous sharp features around ν_H in the spectrum of IV and absent for I arise from the protons on the fluoroanilide ring. The features symmetrically placed around ν_F in IV and absent in the spectrum for I arise from the fluorine substituent. Previously,[46] as well as in this investigation, we have observed that a temperature of 40 K is optimal for ENDOR of nitroxyl spin-labels. Above 40 K, the EPR and ENDOR absorption amplitudes decrease; at temperatures below 40 K, the EPR spectrum vanishes, at least for spin-labels in hydroxylic media. This stands in contrast to the observations of others[47] in which a temperature of 252 K was optimal for ENDOR of spin-labels incorporated into host organic crystals.

principal values of the g matrix, $g_\parallel$ and $g_\perp$ are measured at values of $\mathbf{H}_0$ corresponding to extrema in the first-derivative spectrum. Analogously for ENDOR, $A_\parallel$ and $A_\perp$ are measured at values of the rf field near the extremum points of the first-derivative spectrum. Similar observations have been noted by O'Malley and Babcock.[44]

Results and Discussion

A. ENDOR of Spin-Labeled Fluoroanilides. 1. The Electron–Fluorine Hyperfine Interaction. Figure 4 illustrates the first-derivative ENDOR spectrum of the parent spin-label compound, structure I, and of its *p*-fluoroanilide derivative, structure IV. This comparison directly identifies resonance features that belong to the protons and the fluorine substituent of the *p*-fluoroanilide group. The symmetrically placed features occurring in the 11.0–13.0- and 15.5–17.5-MHz range are common to both compounds and, therefore, are ascribed to the methyl and vinylic protons of the tetramethylpyrrolinyl ring. They exhibit ENDOR shifts greater than 0.5 MHz.[45] The proton resonances of the anilide group of structural interest are observed within ±0.5 MHz of the free proton frequency and are resolved because of the use of a perdeuterated solvent and a modulation depth of the rf field of less than 10 kHz. Similarly, the resonances due to the fluorine

(43) Coope, J. A. R. *Chem. Phys. Lett.* **1969**, *3*, 589–593.
(44) (a) O'Malley, P. J.; Babcock, G. T. *J. Chem. Phys.* **1984**, *80*, 3912–3913. (b) O'Malley, P. J.; Babcock, G. T. *J. Am. Chem. Soc.* **1986**, *108*, 3995–4001.
(45) With use of selectively deuterated samples of compound I, we have established that the sharp ENDOR resonance feature with an ENDOR shift of ~1.95 MHz belongs to the vinylic proton while the broader resonances with an ENDOR shift of ~3.1 MHz belong to the methyl protons: Mustafi, D., Wells, G. B., Makinen, M. W., unpublished observations.
(46) Makinen, M. W. D. Phil. Thesis, Oxford University, Oxford, U. K., 1976, pp 352.
(47) Ohzeki, F.; Kispert, L. D.; Arroyo, C.; Steffan, M. *J. Phys. Chem.* **1982**, *86*, 4011–4016.

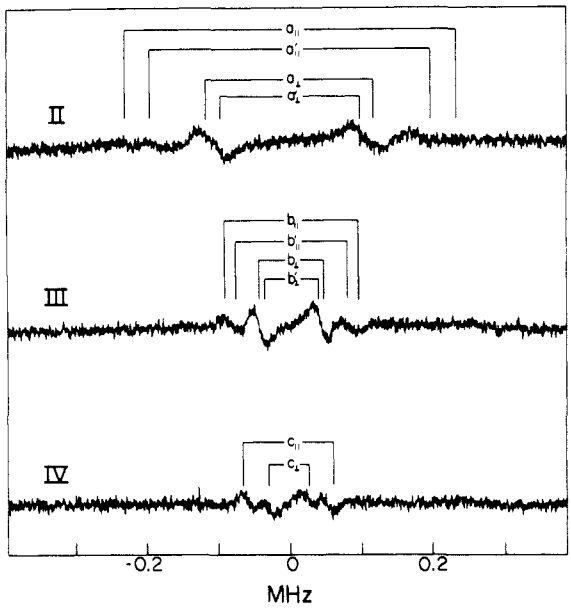

Figure 5. Fluorine ENDOR spectra of spin-labeled fluoroanilides under the isotropic approximation of randomly oriented molecules. The horizontal axis presents the ENDOR shift ($\nu_\pm - \nu_F$) in MHz. Roman numerals correspond to spectra of structures II–IV, respectively. In each case H_0 was applied to setting B, the central region of the EPR spectrum indicated in Figure 2. The spectra illustrate the dependence of the ENDOR shift as the fluorine substituent occupies different positions on the aniline ring. The features $a_\parallel$, $a'_\parallel$, $a_\perp$, and $a'_\perp$ for II are assigned to parallel and perpendicular hfc components of the ortho fluorine substituent in two different conformations of the anilide ring. Similarly, the less well-resolved pairs of features $b_\parallel$, $b'_\parallel$, $b_\perp$, and $b'_\perp$ of III are identified indicating two different conformations of the meta fluorine substituent. In contrast, the unique position of the para fluorine substituent relative to the spin-label moiety of IV produces only two pairs of features, $c_\parallel$ and $c_\perp$. The assignment of the ENDOR features is indicated with aid of the stick diagrams. The values of the splittings, as presented in Tables I and II, were determined directly on the spectral trace independently for each isomer in order to assess the general accuracy of assigning the ENDOR shifts for each set of nuclei common to the three isomers.

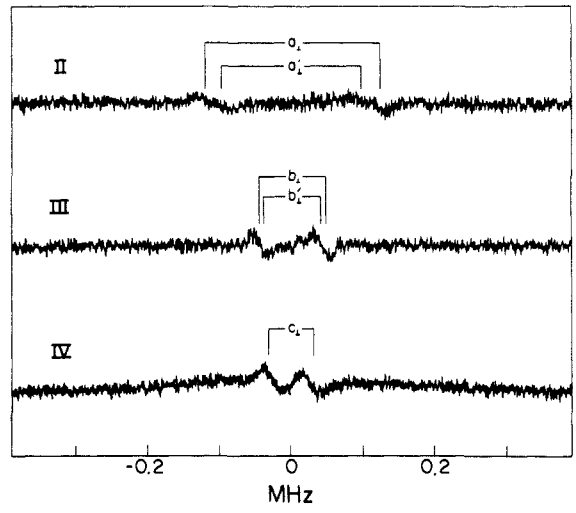

Figure 6. Fluorine ENDOR spectra of spin-labeled fluoroanilides with H_0 applied to the low-field absorption of the EPR spectrum of the nitroxyl group. The splittings of the features $a_\perp$, $a'_\perp$, $b_\perp$, $b'_\perp$, and $c_\perp$ are identical with the ENDOR splittings of Figure 5 observed here with H_0 applied to setting A, the low-field edge of the EPR spectrum with $m_I = \pm 1$. The presence of perpendicular ENDOR features for this setting of H_0 indicates that r for each fluorine lies at least very nearly exactly in the plane of the pyrrolinyl ring.

Table I. Summary of Fluorine ENDOR Results of Spin-Labeled Fluoroanilides[a]

fluorine position	$A_\parallel$	$A_\perp$	$A_\parallel^D$	$A_\perp^D$	A_{iso}	r (Å)[b]
a	0.50	−0.26	0.50	−0.25	−0.010	6.6 ± 0.3
a′	0.40	−0.20	0.40	−0.20	−0.002	7.2 ± 0.3
b	0.18	−0.10	0.19	−0.09	−0.004	9.3 ± 0.7
b′	0.17	−0.08	0.16	−0.08	−0.001	9.7 ± 0.9
c	0.12	−0.06	0.12	−0.06	0.000	10.6 ± 1.3

[a] Hfc constants are indicated in units of MHz. [b] An uncertainty in hfc constants of approximately ±0.02 MHz is included in the calculation of electron–nucleus distances.

substituent are found to within ±0.5 MHz of the free nuclear frequency of fluorine and are clearly distinguishable against the background of the proton resonances of the spin-label moiety. As is seen in Figure 4, the resonance bands due to the fluorine and protons of the anilide group do not overlap. Similar observations were also made for the isomeric anilides II and III.

Figure 5 illustrates in greater detail ENDOR absorptions due to the fluorine substituent for each of the three isomeric anilides. The condition of H_0 applied to setting B defined in Figure 2 invokes our isotropic approximation, as discussed above, and yields the largest peak-to-peak amplitudes. We identify these features as the buildup of intensity around frequencies corresponding to the principal values of the hfc components. In Figure 5 the spectrum of IV exhibits only two pairs of features detectable within the limitations of gain imposed by our spectrometer. With a planar amide group, the position of the para fluorine substituent is unique and is independent of the relative conformation of the anilide ring to the plane of the nitroxyl group. We conclude that the observation of only two pairs of ENDOR features is indicative of an axially symmetric electron–fluorine hfc interaction. A detailed comparison of the spectra of isomers II and III in Figure 5 indicates sets of ENDOR absorptions that are partially overlapping but nonetheless are distinctly detected. Isomers II and II each may be expected to have two conformers with respect to the fluorine substituent related by a rotation around the anilide N–C bond. Since other ENDOR absorptions due to the fluorine substituent were not detected, we conclude that the observation of pairs of features are due to the two rotationally derived conformers. The two sets of ENDOR absorptions are most clearly resolved for isomer II. There are two pairs of features within each set, and we consequently conclude that the hf interaction is axially symmetric for each rotational conformer, as for the para fluorine substituent of IV.

Within our isotropic approximation of the EPR spectrum of nitroxyl spin-labels, we have designated the pairs of features in Figure 5 as belonging to the parallel and perpendicular hfc components according to the shape of the resonance features and the magnitudes of the splittings predicted by eq 3 for $\alpha = 0°$ and $\alpha = 90°$, respectively. This assignment is confirmed in Figure 6 with H_0 applied at the low-field EPR absorption, designated as setting A. This setting of H_0 selects molecular orientations such that the plane of the pyrrolinyl ring is perpendicular to H_0, a condition that gives rise to perpendicular ENDOR splittings of nuclei coincident with the molecular x,y plane. In each spectrum in Figure 6, the splittings are identical with the splittings labeled $a_\perp$, $b_\perp$, and $c_\perp$ in Figure 5, and features corresponding to $a_\parallel$, $b_\parallel$, or $c_\parallel$ of Figure 5 are not observed. Furthermore, isomers II and III each exhibit sets of closely spaced pairs of features while isomer IV exhibits only one pair of features consistent with its uniquely positioned fluorine substituent. It is of interest to note that the values of the splittings in Figure 6 and their counterparts in Figure 5 remain independent of H_0. However, the amplitudes of the ENDOR features were dependent upon the H_0 setting according to the intensity of the EPR absorption at settings A and B.

We have summarized in Table I the values of the principal hfc components of the fluorine substituent for each isomer and have indicated the corresponding electron–fluorine separation r evaluated on the basis of eq 3.

2. The Electron–Proton Hyperfine Interaction. The proton ENDOR spectra are analyzed according to the same procedure applied to the fluorine spectra. Because of the absence of parallel features with H_0 applied to the low-field EPR absorption, it is more straightforward to analyze first the proton ENDOR spectra

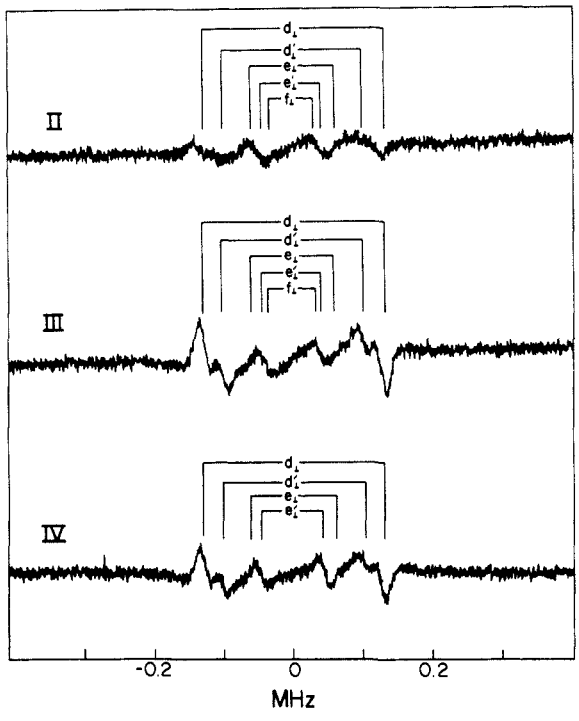

Figure 7. Proton ENDOR spectra of spin-labeled fluoroanilides with $\mathbf{H}_0$ applied to the low-field absorption of the EPR spectrum of the nitroxyl group. According to Figures 5 and 6, only perpendicular features are observed with this setting of $\mathbf{H}_0$. The assignment of the pairs of features is discussed in the text.

of isomers II–IV obtained with $\mathbf{H}_0$ applied to the low-field feature of the EPR spectrum designated as setting A (Figure 2). The spectra are illustrated in Figure 7. Spectrum IV in Figure 7 exhibits four well-resolved pairs of resonance features that are directly assigned to protons at the ortho and meta positions of the anilide ring and are labeled d, d′ and e, e′ respectively. In the spectrum of III the features due to the ortho protons (d, d′) exhibit identical splittings as in spectrum IV, indicating that the relative conformations of the anilide ring with respect to the spin-label are preserved. There are weak resonance features in the central region of spectrum III not observed in spectrum IV. These are ascribed to the proton at the para position. In spectrum II the features due to ortho protons are noticeably decreased in amplitude, as expected for an anilide ring with an ortho fluorine substituent.

Figure 8 illustrates the proton ENDOR spectra of II–IV with $\mathbf{H}_0$ applied at setting B. As for the ^{19}F ENDOR spectra under the isotropic approximation, both parallel and perpendicular ENDOR absorptions are observed. Comparison of the spectra in Figure 8 with those in Figure 7 shows that all of the absorptions identified in Figure 7 are preserved with identical ENDOR shifts. In addition, new ENDOR features are observed that we attribute to the parallel absorptions of protons in the ortho positions. The expected parallel ENDOR shifts for protons e and f at the meta and para positions cannot be clearly assigned because of overlap with the more prominent resonance features of the ortho protons designated as d.

Similarly to the ENDOR features of the fluorine substituent of isomers II–IV, sets of pairs of absorption features are resolved for each class of protons. This is best illustrated by the ENDOR spectrum of isomer III in Figure 8 in which parallel and perpendicular absorptions are identified for the ortho protons. Since a total of only four pairs of features were detected for protons d and d′, the hf interaction is axially symmetric. We correspondingly assume that the ENDOR splittings of the other classes of protons exhibit similarly axial symmetry although we cannot demonstrate this relationship directly since the parallel splittings $e_\parallel$, $e'_\parallel$, and $f_\parallel$ overlap with other, more intense ENDOR resonances.

In Table II we have summarized the observed principal hfc components for each class of aromatic anilide proton. Correspondingly, the electron–proton distances are listed, calculated on the basis of eq 3. We have not been able to detect the ENDOR splittings of the amide hydrogen with use of CD_3OD as solvent,

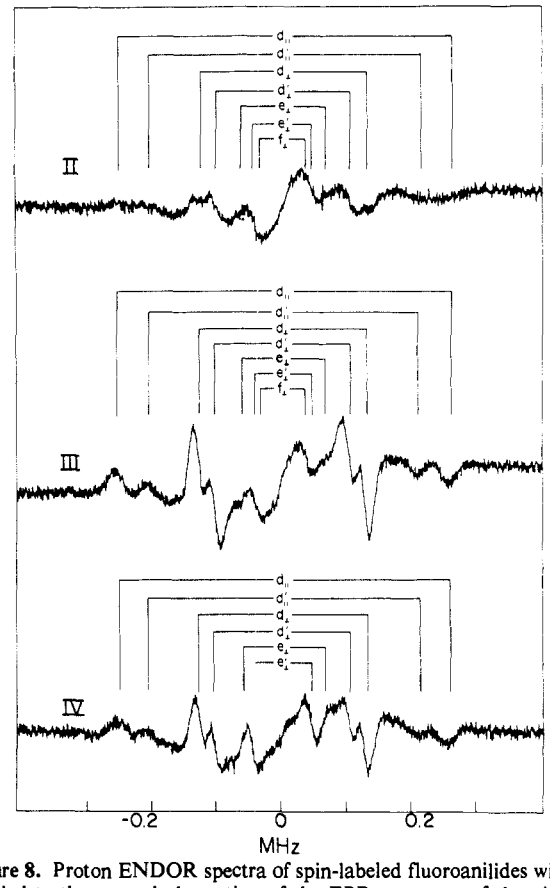

Figure 8. Proton ENDOR spectra of spin-labeled fluoroanilides with $\mathbf{H}_0$ applied to the central absorption of the EPR spectrum of the nitroxyl group. Comparable to the fluorine spectra, we expect the two ortho and the two meta protons to have different sets of values for their principal hfc components. Features from five protons on the aniline ring should appear in II and III, while features from four protons should appear in IV. The five protons expected in the spectrum of III, for example, could give rise to a maximum of five pairs of parallel and five pairs of perpendicular features. This level of resolution is not observed. Based on the spectral changes which occur as the fluorine occupies different positions on the anilide ring, we assign features d and d′ to ortho protons, e and e′ to meta protons, and f to the para proton. Some uncertainty for the assignments of d and d′ remains because of the potential overlap of $e_\parallel$, $e'_\parallel$, and $f_\parallel$ with $d_\perp$ and $d'_\perp$. This uncertainty is removed on the basis of Figure 7 in which the parallel features are absent.

Table II. Summary of Proton ENDOR Results of Spin-Labeled Fluoroanilides[a]

proton position and isomer	$A_\parallel$	$A_\perp$	$A_\parallel^D$	$A_\perp^D$	A_{iso}	r (Å)
2-fluoroanilide						
d	0.51	−0.27	0.52	−0.26	−0.007	6.7 ± 0.3
d′	0.43	−0.22	0.43	−0.22	−0.003	7.2 ± 0.3
e		−0.12				8.8 ± 0.5
e′		−0.10				9.2 ± 0.7
f		−0.08				9.9 ± 1.0
3-fluoroaniline						
d	0.52	−0.27	0.52	−0.26	−0.006	6.7 ± 0.3
d′	0.41	−0.22	0.42	−0.21	−0.006	7.2 ± 0.3
e		−0.12				8.7 ± 0.5
e′		−0.09				9.7 ± 0.7
f		−0.07				10.2 ± 1.0
4-fluoroanilide						
d	0.51	−0.26	0.52	−0.26	−0.006	6.7 ± 0.3
d′	0.42	−0.21	0.42	−0.21	−0.002	7.2 ± 0.3
e		−0.12				8.8 ± 0.5
e′		−0.10				9.3 ± 0.7

[a] See Table I for units and constraints.

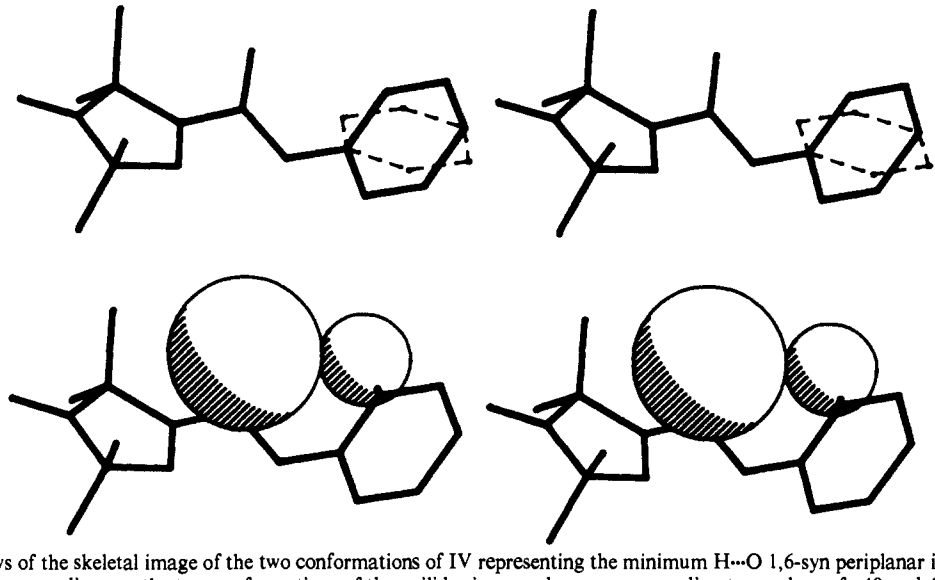

Figure 9. Stereoviews of the skeletal image of the two conformations of IV representing the minimum H···O 1,6-syn periplanar interaction of the carbonyl oxygen atom. In the upper diagram the two conformations of the anilide ring are shown corresponding to χ values of −49 and 47°. In the lower diagram the volume described by the van der Waals radii of the carbonyl oxygen and of the proton at the ortho position is indicated for the conformer with $\chi = -49°$ to illustrate the steric interaction preventing a coplanar conformation of the two ring systems.

presumably since the exchange rate of amide protons of anilides with solvent molecules can be fast[48] with respect to the shortest time of mixing the spin-labeled anilides and freezing of the solvent in our experiments. On the other hand, protonated solvent media yielded broad ENDOR resonance features corresponding to the free matrix signal that obscured the splittings of the anilide protons described here.

B. Molecular Modeling of the Conformation of Spin-Labeled Anilides. We have compared the ENDOR determined values of r in Tables I and II for electron–fluorine and electron–proton separations with expectations based on molecular models of each spin-labeled fluoroanilide. The structure of each fluoroanilide isomer was constructed as described above from molecular fragments. We have restricted the modeling to conform to the nonhydrogen atomic skeleton of the spin-label moiety defined in X-ray studies.[25,32] In the structure of 2,2,5,5-tetramethylpyrroline-1-oxyl-3-carboxamide, the carbonyl group deviates slightly from the plane of the pyrrolinyl ring, and this structural feature was preserved in molecular modeling data. To join the fluoroanilide group to the spin-label, a C–N–C valence angle of 120° was imposed.

The chemical bonding structure of the spin-labeled anilides of Figure 1 suggests the presence of π-conjugation extending from the olefinic bond in the pyrrolinyl ring, through the amide linkage, into the aromatic group. this should tend to stabilize a coplanar conformation of the pyrrolinyl and anilide rings. However, a coplanar conformation cannot be sterically accommodated since the 1,6-syn-periplanar steric interaction between the carbonyl oxygen and an ortho hydrogen or fluorine prevents coplanarity of the two ring systems.[49] Therefore, we assume for construction of the model that the magnitude of χ will take the minimum value that is consistent with the steric constraints imposed by this interaction. A van der Waals radius of 1.5 Å for the carbonyl oxygen and 0.9 Å for hydrogen[50] sets the minimum nonbonded H···O contact distance at 2.4 Å for the 1,6-syn interaction in isomers II, III, and IV. The resultant values of χ are −49 or 47°, as illustrated in Figure 9. For isomer II, however, the F···O 1,6-syn interaction sets the minimum values of χ to −70 or 68° because of the larger radius of a fluorine substituent (1.5 Å) compared to that of hydrogen.

Comparison of the ENDOR determined values of r with those obtained from molecular modeling will be sensitive to the method of assigning the effective dipole–dipole distance within the molecule. The quantity $(l^2 + d^2)^{1/2}$ has been employed as an approximation of the dipole–dipole interaction distance of nitroxyl spin-labels[47,53] since the unpaired spin is distributed primarily in

Table III. Comparison of Values of Electron–Nucleus Separations Based on ENDOR and Molecular Modeling Studies of Spin-Labeled Fluoranilides

		electron–nucleus separation[b]		
			molecular molding[c]	
substituent	position[a]	ENDOR		
fluorine	a	6.6 ± 0.3	6.92	6.64
	a′	7.2 ± 0.3	7.33	7.53
	b	9.3 ± 0.7	9.24	9.08
	b′	9.7 ± 0.9	9.74	9.91
	c	10.6 ± 1.3	10.51	10.51
proton[d]	d	6.7 ± 0.3		
		6.7 ± 0.3	6.74	6.54
		6.7 ± 0.3		
	d′	7.2 ± 0.3		
		7.2 ± 0.3	7.34	7.52
		7.2 ± 0.3		
	e	8.8 ± 0.5		
		8.7 ± 0.5	9.12	8.98
		8.8 ± 0.5		
	e′	9.2 ± 0.7		
		9.7 ± 0.7	9.58	9.73
		9.3 ± 0.7		
	f	9.9 ± 1.0	10.30	10.30
		10.2 ± 1.0		

[a] Positions are indicated in Table I for fluorines and in Table II for protons. [b] Distances are indicated in Ångstrom units. Distances obtained in molecular modeling studies are calculated for a value for ρ_N of 0.5. [c] The left- and right-hand sets of values correspond to separations calculated for the minimum 1,6-syn periplanar interactions with values of $\chi = -70$ and 68° for F···O and $\chi = -49$ and 47° for H···O. [d] For each position d,d′, e,e′, and f, the ENDOR determined electron–proton separations are listed for isomers II, III, and IV, respectively.

(48) Takahashi, T.; Mamoru, N.; Masamichi, T. *Bull. Chem. Soc. Jpn.* **1978**, *51*, 1988–1990.
(49) In acetanilide the aromatic ring makes an angle of 18° with the plane of the amide group.[28]
(50) Our value for the van der Waals radius of an aromatic hydrogen is a compromise between that suggested by Bondi[51] and Gavezotti[52] (1.0–1.2 Å) and the apparent radius of 0.8 Å observed in the 2.26-Å interaction between the carbonyl oxygen and the nearer ortho hydrogen in acetanilide.[28]
(51) Bondi, A. *J. Phys. Chem.* **1964**, *68*, 441–451.
(52) Gavezotti, A. *J. Am. Chem. Soc.* **1983**, *105*, 5220–5225.
(53) Calder, A.; Forester, A. R., James, P. G.; Luckhurst, G. R. *J. Am. Chem. Soc.* **1969**, *91*, 3724–3727.

the p_z orbitals of the nitrogen and oxygen atoms of the nitroxyl group. In this expression d = 1.4 Å and represents the distance between the point dipoles of the partial charges in each of the orbital lobes above and below the plane.[54] With l as the model derived distance between the nitroxide nitrogen and the nucleus in question, the values of $(l^2 + d^2)^{1/2}$ were uniformly smaller than the corresponding ENDOR determined values of r for the most accurately assigned ENDOR splittings. On the other hand, l as the internuclear distance to the nitroxyl oxygen invariably yielded values of $(l^2 + d^2)^{1/2}$ larger than the ENDOR determined values of r. This result simply reflects the circumstance that the unpaired spin is distributed between the nitrogen and oxygen atoms and is not confined to a p_z orbital of the nitroxyl nitrogen or of the oxygen alone. We, therefore, assigned the coordinates of the *effective* electronic point dipole of the nitroxyl group according to eq 5 for $\rho_N = \rho_O = 0.5$ to estimate the electron–nucleus distance in molecular models.

In Table III we have compared the electron–fluorine and electron–proton separations determined on the basis of ENDOR data to those calculated from molecular models. Evaluation of the electron–proton separations for the ortho hydrogens supports the choice of 0.5 for the values of ρ_N. For ρ_N = 0.8, the distance to the closer aromatic hydrogen in the models is 6.39 Å. This value does not account satisfactorily for the principal dipolar hfc components obtained from the ENDOR data, particularly for isomers III and IV which exhibited the best resolved ENDOR features. On the other hand, the less well-resolved ENDOR features belonging to the more distant meta and para aromatic hydrogens make them unsuitable for evaluating the best choice of r_e in eq 5. In addition, the value of 0.5 for ρ_N is in good agreement with the finding by Davis et al.,[36a] who report values of ρ_N ranging from 0.42 to 0.48 on the basis of ab initio calculations for planar H_2NO. We have not attempted in this investigation to define r_e more accurately but note that this may require small adjustments for spin-labels of different structure and in solvents at different polarity since the isotropic nitrogen hfc constant is weakly sensitive to these factors.[12,37] The values of r determined on the basis of ENDOR data and on the basis of molecular models summarized in Table III agree to within 5%. This agreement confirms the assignment of values of the principal hfc components from ENDOR splittings on the basis of the simulations described above. Also, it demonstrates that the ENDOR spectra of nitroxyl spin-labels can be accurately interpreted on the basis of our isotropic approximation.

Although the molecular models were not constructed on the basis of ENDOR results, it is possible to extend this approach to evaluate the range of conformations of the anilide ring that are compatible with the ENDOR data. This was done by carrying out a conformational search[31] for the range of χ consistent with limits set by nonbonded interactions and the estimated errors associated with each ENDOR-determined value of r. The results are summarized in Figure 10. The upper part compares in the form of a Newman diagram the relative conformations of the anilide ring that are limited by the 1,6-syn periplanar H···O and F···O interactions. The lower part illustrates the range of χ that remains compatible with the ENDOR determined values of r and its associated errors for isomer IV. It is evident that the constraints imposed by ENDOR data significantly restrict the conformational range of χ compared to that allowed by steric interactions alone and that the ENDOR constrained range of χ is near those values consistent with the minimum 1,6-syn periplanar H···O interactions of the carbonyl oxygen and ortho aromatic hydrogens. This result then suggests that the tendency toward π-conjugation and coplanar ring orientations of the spin-labeled fluoroanilide is strongly favored and that the actual conformation is likely to be that with the shortest nonbonded H···O interactions.

C. General Conclusions. The ENDOR shifts assigned to features in the fluorine and proton ENDOR spectra are, within

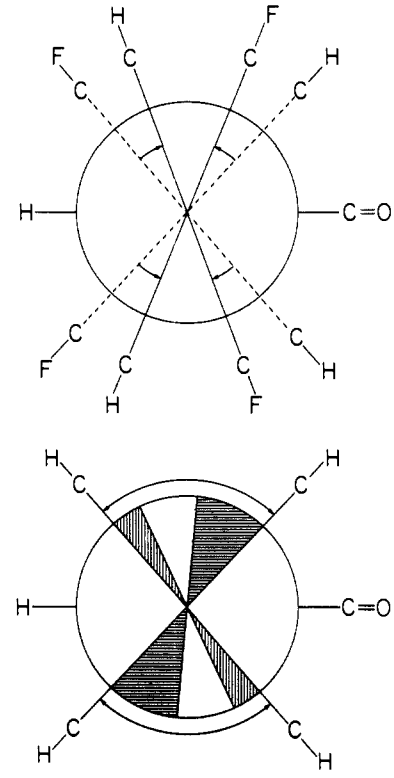

Figure 10. Newman diagrams illustrating the range of values of χ in spin-labeled fluoroanilides. Both diagrams are drawn to correspond to a projection down the (aromatic) C–(amide) N bond in which the central point represents the aromatic C atom and the circle represents the amide N. In the upper diagram the positions are indicated for values of χ = −70 and 68° for the minimum 1,6-syn periplanar F···O interactions and for values of χ = −49 and 47° for the H···O interactions. In the lower diagram, the sterically accessible range of χ is indicated for isomer IV. The shaded sectors correspond to the range of χ compatible with the ENDOR determined values of r for electron–proton separations and their associated errors at the two ortho positions. The range of conformations of the aromatic ring that are constrained only by steric interactions is indicated by arrows. The shaded sectors correspond to the range of conformations that are compatible with both van der Waals nonbonded interactions and the ENDOR-determined values of r (Table III). The conformation search that defined these ranges used the error limits for the ENDOR-determined values of r for the meta protons and para fluorine shown in Table III. For ortho protons d and d′, the error limits for the values of r were employed so as to reflect the observation that the two ortho protons were found at distinguishably different distances by ENDOR. The range for a d proton was 6.4–6.9 Å while that for a d′ proton was 7.0–7.5 Å.

measurement, independent of the magnetic field setting $\mathbf{H}_0$. This observation is consistent with the use of an isotropic approximation for determining the principal hfc values with the $\mathbf{H}_0$ setting at position B shown in Figure 2. Because of negligible EPR absorption anisotropy relative to the single-crystal EPR line width for the m_I = 0 region of the EPR spectrum of nitroxyl spin-labels, the prominent features that appear in the ENDOR spectra are due to extrema in the values of the hfc components rather than to a subset of orientations contributing to the position selected for microwave saturation of the EPR spectrum. Fluorine ENDOR of isomer IV provides the best support for this conclusion.

Microwave saturation at position A or the low-field edge of the EPR spectrum, as defined in Figure 2, provides the best defined selection of molecular orientations for ENDOR. Absence of parallel ENDOR features for this setting requires that r is not oriented perpendicularly to the plane of the spin-label pyrrolinyl ring. Our simulations of ENDOR spectra in Figure 4 from an axially symmetric EPR center with axially symmetric hf interactions suggest that an angle ≤25° between the plane of the pyrrolinyl ring and r for the protons and fluorines of the aniline moiety in the molecular models is compatible with the absence of the parallel features and the presence of perpendicular features

(54) (a) Shulman, R. G.; Rahn, R. O. *J. Chem. Phys.* **1966**, *45*, 2940–2946. (b) Pullman, A.; Kochanski, E. *Int. J. Quantum Chem.* **1967**, *1S*, 251–259.

in ENDOR spectra when H_0 is set to position A of the EPR spectrum. In fact, sample calculations based on the atomic coordinates derived from modeling studies show that the largest deviation of r from the molecular plane of the spin-label is ~21° and corresponds to the electron-fluorine separation of 7.2 Å of the ortho-fluorinated derivative (cf. Table III). This comparison provides support for the adequacy of the model chosen for spectral simulations in this study. A more quantitative estimate of this angle, however, depends either on the detection of some feature for which the ENDOR shift depends on H_0 or on simulation of the ENDOR spectra with a more detailed approach to modeling of the intensities of the first derivative features and the single-crystal EPR line widths, perhaps by incorporating the anisotropy of relaxation effects.[55]

The parallel and perpendicular features in the fluorine ENDOR spectra of IV exhibit line widths of approximately 20 kHz. Line widths of other features were also approximately 20 kHz although overlap of features made their measurement difficult. The line width of the ENDOR resonance feature limits the accuracy for separating classes of nuclei on the basis of r. For a peak-to-peak separation of 20 kHz for the detectable ENDOR absorptions, we may expect to resolve the resonance features of classes of protons for which the electron-nucleus separation differs by about 0.2 Å for r values of about 7 Å. For separations of ~10 Å, the values of r must differ by ~1 Å for 20-kHz line widths. This level of resolution is confirmed experimentally at the 7-Å range by the observation of distinguishable features from the two ortho protons in III and IV and at the 10-Å range by the distinguishable features from the meta and para protons of III and the meta protons of IV. Because of the similar g_n values of proton and fluorine nuclei, these estimates are approximately correct for fluorine as well.

The accuracy of measurements of r from hfc constants can be assessed on the basis of the molecular models. As the assignment of the coordinates of the electronic point-dipole of the nitroxyl group was changed from $\rho_N = 0.8/\rho_O = 0.2$ to $\rho_N = 0.5/\rho_O = 0.5$, the values of r calculated from hfc constants and from models disagreed by less than 5%. For instance, for fluorine the average deviation and root-mean-square of the deviation of r were -0.29 and 0.33 Å for $\rho_N = 0.8$ and 0.06 Å and 0.18 Å for $\rho_N = 0.5$, respectively. The assignment of $\rho_N = 0.5/\rho_O = 0.5$, in general, yielded the best agreement between the ENDOR determined values of r and those calculated from molecular models.

It is, thus, evident that ENDOR spectroscopy of spin-labeled compounds provides a generally applicable method of noncrystallographic structure determination of molecules in frozen solutions or polycrystalline systems through measurements of electron-nucleus distances in the range from 5 to 11 Å for protons and fluorines. In addition to their extensive use in EPR spectroscopy,[9-12] spin-labels may find another role in magnetic resonance as probes of molecular geometry through ENDOR spectroscopy to provide an accurate noncrystallographic method for structure determination of immobilized molecules in solution.

(55) (a) Narayama, P. A., Bowman, M. K.; Becher, D.; Devan, L. *J. Chem. Phys.* **1977**, *67*, 1990-1996. (b) Kevan L. Narayana, P. A.; Toriyama, K.; Iwasaki, M. *J. Chem. Phys.* **1979**, *70*, 5006-5014.

Nuclear Magnetic Resonance Study of the Molecular and Electronic Structure of the Stable Green Sulfhemin Prosthetic Group Extracted from Sulfmyoglobin

Mariann J. Chatfield, Gerd N. La Mar,* W. O. Parker, Jr., Kevin M. Smith, Hiu-Kwong Leung, and Ian K. Morris

Contribution from the Department of Chemistry, University of California, Davis, California 95616. *Received January 25, 1988*

Abstract: The ^{1}H NMR spectral characteristics of the stable green heme extract sulfhemin C from the terminal alkaline equilibration product of sulfmyoglobin have been investigated in order to completely define its molecular structure and to shed light on the nature of metal-prosthetic group π-bonding as reflected in the contact shift pattern in paramagnetic ferric complexes. A complete stereospecific assignment of the ^{1}H NMR spectrum of the low-spin dicyano complex was effected by a combination of isotope labeling, spin decoupling, analysis of differential paramagnetic dipolar relaxation, and nuclear Overhauser effect, which confirmed that all functional groups of the precursor hemin are retained with the exception of the saturation of pyrrole B to form a cyclic thiolene. The assignments depended upon the use of a viscous solvent to render NOEs detectable, but it is shown that the combination of NOEs and metal-centered relaxation is sufficient to yield assignment without recourse to isotope labeling, opening the possibility for assignment of the spectra of natural low-spin ferric chlorin complexes. The dicyanosulfhemin C contact shift pattern is shown to reflect primarily π-bonding with the highest filled π MO of the chlorin, as found previously for hemin, except that its metal spin is symmetry-restricted to interacting solely with the pyrroles cis to the saturated ring. The raising of the iron d orbital degeneracy by the ring B saturation provides the explanation of why low-spin ferric sulfhemin C, in contrast to hemin, experiences a negligible perturbation of the contact shift pattern upon incorporation into a protein and why the contact shift pattern does not uniquely identify the saturated pyrrole in a chlorin. The assignment by isotope labeling of the peripheral methyl signals of the high-spin ferric bis(dimethyl sulfoxide) complex of sulfhemin C confirms an electronic structure very similar to that observed upon incorporation into a protein matrix. We also confirm that the unique and sharply attenuated 3-methyl contact shift identifies the saturated ring as pyrrole B and that the assignment of high-spin ferric chlorin peripheral methyl signals will yield the identity of the saturated pyrrole(s).

Sulfhemoglobin is a green pigmented nonfunctional form of hemoglobin that can occur under physiological conditions.[1] Sulfmyoglobin, SMb, is an analogous substance, formed in the laboratory by the sequential reaction of myoglobin with H_2O_2 and thiol, which has been frequently used to facilitate the study of the structural modification of sulfhemoglobin.[2-6] Early work on SMb revealed that a sulfur atom is incorporated into the hemin

(1) Park, C. M.; Nagel, R. L. *N. Engl. J. Med.* **1984**, *310*, 1579-1584.

(2) Berzofsky, J. A.; Peisach, J.; Blumberg, W. E. *J. Biol. Chem.* **1971**, *246*, 3367-3377.

(3) Berzofsky, J. A.; Peisach, J.; Blumberg, W. E. *J. Biol. Chem.* **1971**, *246*, 7366-7372.

0002-7863/88/1510-6352$01.50/0